Title

Controlled tubulogenesis from dispersed ureteric bud-derived cells using a micropatterned gel

Journal

Journal of Tissue Engineering and Regenerative Medicine, 10(9)

ISSN

1932-6254

Authors

Hauser, Peter V
Nishikawa, Masaki
Kimura, Hiroshi
et al.

Publication Date

2016-09-01

DOI

10.1002/term.1871

Peer reviewed

JOURNAL OF TISSUE ENGINEERING AND REGENERATIVE MEDICINE
J Tissue Eng Regen Med (2014)
Published online in Wiley Online Library (wileyonlinelibrary.com) **DOI:** 10.1002/term.1871

RESEARCH ARTICLE

Controlled tubulogenesis from dispersed ureteric bud-derived cells using a micropatterned gel†

Peter V. Hauser[1,2]*, Masaki Nishikawa[1,2], Hiroshi Kimura[3], Teruo Fujii[3] and Norimoto Yanagawa[1,2]
[1]*Renal Regeneration Laboratory, VAGLAHS at Sepulveda, North Hills, CA, USA*
[2]*David Geffen School of Medicine, University of California at Los Angeles, CA, USA*
[3]*Institute of Industrial Science, University of Tokyo, Japan*

Abstract

Developmental engineering is a potential option for neo-organogenesis of complex organs such as the kidney. The application of this principle requires the ability to construct a tubular structure from dispersed renal progenitor cells with defined size and geometry. In this present study we report the generation of tubular structures from dispersed ureteric bud cells *in vitro* by using a micropatterned gel. Dispersed CMUB-1 cells, a mouse ureteric bud-derived cell line, or mIMCD cells, a mouse collecting duct-derived cell line, were suspended in collagen I and seeded into an agarose-based micropatterned gel. We found that within 24–36 h of incubation, the cells developed a tubular structure that conformed to the geometry of the micropattern of the gel. The lumen formation of the tubular structure was confirmed by immunohistochemical staining and observed by confocal microscopy. We found that higher concentrations of collagen I negatively influenced the efficiency of tubular formation. Tubule formation in CMUB-1, but not mIMCD, cells was positively influenced by the addition of aldosterone (10, 50 and 200 μg/ml), FGF (50 and 100 μg/ml) and fibronectin (10 and 50 μg/ml) to the growth medium. We further demonstrated the functionality of the generated tubes by *in vitro* budding, which was induced by growth factors, such as glial cell-derived neurotrophic factor (GDNF) or fibroblast growth factor 7 (FGF7), in the presence of beads soaked with the activin A inhibitor follistatin. Our current study thus demonstrates the possibility of constructing a functional tubular structure from dispersed ureteric bud cells *in vitro* in a controlled manner. Copyright © 2014 John Wiley & Sons, Ltd.

Received 4 February 2013; Revised 15 November 2013; Accepted 2 January 2014

Keywords **tissue engineering; kidney development; ureteric bud; tubulogenesis; organogenesis; developmental engineering**

1. Introduction

Renal transplantation and dialysis are currently the only options to treat end-stage renal disease (ESRD), the permanent loss of kidney function. Regenerative medicine aims to expand the therapeutic options by developing alternative strategies to overcome the limitations associated with these therapies (Little, 2006). The option of *de novo* generation of a mature kidney by tissue engineering seems unlikely, due to its complex architecture and the many cell types in the kidney. A more realistic approach is to construct the structurally much simpler embryonic kidney and to employ the principles of developmental engineering to facilitate a process of self-organized growth from progenitor cells similar to organogenesis (Basu and Ludlow, 2012; Lenas *et al*., 2009).

The kidney, like many organs, develops from a tube that grows into the surrounding mesenchymal tissue and branches into a tree-like structure. In the case of the kidney, the tube is an outgrowth of the Wolffian duct, called the ureteric bud (UB), and the surrounding mesenchymal tissue is called metanephric mesenchyme (MM); together they form the embryonic kidney, called the metanephros (Saxen, 1987). Through reciprocal signalling between the UB and the MM, a complex process of differentiation takes

**Correspondence to: Peter V. Hauser, UCLA David Geffen School of Medicine, VAGLAHS at Sepulveda, Renal Regeneration Laboratory, 16111 Plummer Street, Building 7, Room D-110, North Hills, CA 91343, USA. E-mail: pvhauser@ucla.edu*
†*Parts of this study were presented at the American Society of Nephrology meeting in 2011 and published as an Abstract.*

place that includes the development of the collecting duct system from the UB and the mesenchymal–epithelial transition (MET) of the MM to give rise to the remaining nephron structures, starting from Bowman's capsule down to the proximal and distal segments of the renal tubules (Little *et al.*, 2010; Reidy and Rosenblum, 2009; Schmidt-Ott *et al.*, 2006).

Attempts have been made to reconstruct kidney-like tissues by recombining the dissected UB with MM *in vitro*, followed by implantation to further develop *in vivo* (Rosines *et al.*, 2007, 2010). In view of the practical need to use dispersed cultured cells as the starting material, attempts have also been made to create metanephros-like structures *in vitro* by forming aggregates from dispersed UB and MM primary cells (Ganeva *et al.*, 2011; Rosines *et al.*, 2010; Unbekandt and Davies, 2010). Although these studies demonstrated the self-organizational potential of renal progenitor cells *in vitro*, the lack of control over the tubule formation process resulted in organoids with random tubular organization that are incapable of functioning as an excretory organ.

To circumvent this problem, we consider it essential to first construct a UB tube from dispersed UB cells, using a method that allows us to control the geometry of the generated tube. Numerous studies have demonstrated the potential of micropatterned gels to direct the growth of tubular structures *in vitro*. For example, Nelson *et al.* (2006) were able to generate mammary epithelial tubes in a micropatterned gel and control their branching geometry. Using a micropatterned gel, Raghavan *et al.* (2010) produced tubular structures with varying diameters from dispersed endothelial cells.

The aim of our present study was to utilize the self-organization potential of renal progenitor cells to generate tubular structures from dispersed UB cells *in vitro* in a controlled manner. Central to our strategy was a micropatterned gel, which served as a platform to induce tubule formation and define the number, growth and size of the generated tubules.

2. Methods

2.1. Micropatterned mould

A micropatterned platform (mould) was generated by photocatalytic lithography of a SU-8 wafer, as described previously (Evenou *et al.*, 2010; Montagne *et al.*, 2009; Provin *et al.*, 2009) (Figure 1A). The pattern contains 10–20 rectangular cavities with a length (a) of 3 or 6 mm and a width (b) of 50, 75, 100, 125 or 150 μm. The depth of the mould was 100 or 150 μm (Figure 1D). Google SketchUp 8.0 software (sketchup.google.com) was used to design the mould pattern and to generate a virtual three-dimensional (3D) model.

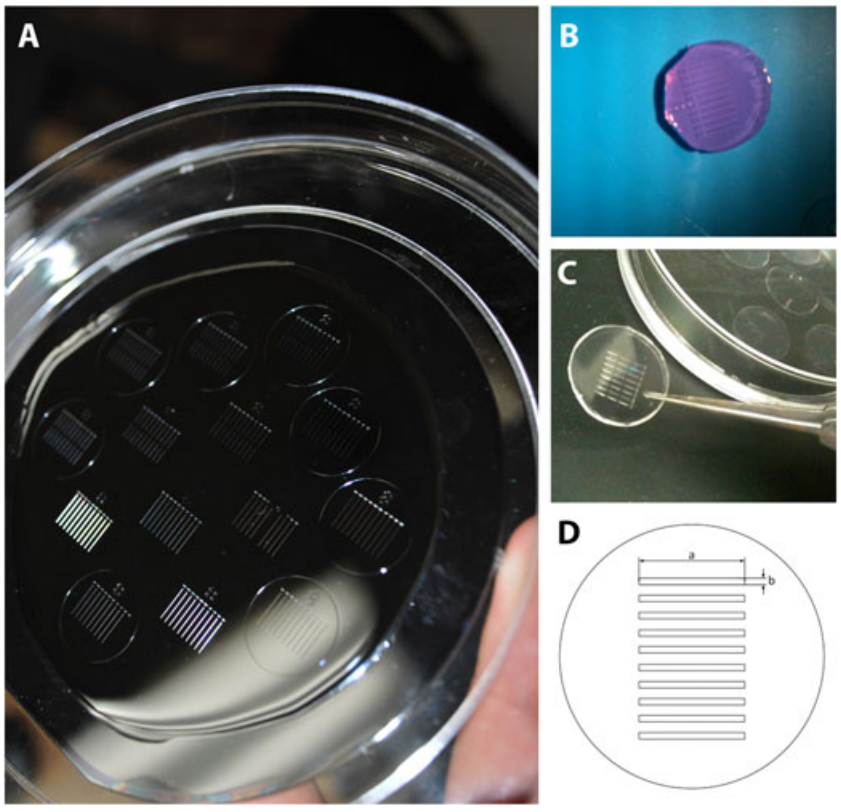

Figure 1. Micropatterned mould. A silicone wafer with a micropattern generated by photolithography (A) was used as the mould to produce agarose gels (B) or PDMS polymers (C) that contained cavities in the shape of the micropattern (D). The dimensions of the cavities were: (a) length 3 or 6 mm; and (b) width 50, 75, 100, 125 or 150 μm

DOI: 10.1002/term

2.2. Micropatterned agarose gel and micropatterned polymer

To produce a micropatterned agarose gel, a 3% agarose solution (Sigma-Aldrich, St. Louis, MO, USA) was prepared in growth medium [Dulbecco's modified Eagle's medium (DMEM) or MEM/F12] under sterile condition and melted. After cooling to 65°C, the agarose was applied to the mould and polymerized at room temperature. The agarose gels were removed from the mould under sterile conditions and used immediately, or stored in an airtight container at 4°C (Figure 1B).

A micropatterned polydimethylsiloxane (PDMS) polymer was produced using the Sylgard 184 Silicon Elastomer Kit (Dow Corning, Midland, MI, USA), according to the manufacturer's recommendations. The reagents were mixed in a ratio of 10:1 and homogenized by stirring. The mixture was then applied to the mould and exposed to a 10% vacuum for 10 min to remove trapped air bubbles. The polymer was cured by baking at 85°C for 2 h. After removal, the micropatterned polymer was washed in 70% ethanol, rinsed in phosphate-buffered saline (PBS) and air-dried in a sterile workbench (Figure 1C).

2.3. Cells and cell culture

The CMUB-1 mouse UB cell line was obtained from Probetex (San Antonio, TX, USA) (Ye *et al*., 2004) and cultured in high-glucose DMEM (Gibco, Invitrogen, Carlsbad, CA, USA) with 10% fetal bovine serum (FBS; Sigma-Aldrich) and penicillin–streptomycin (Pen/Strep; Sigma-Aldrich) in 10 cm non-pyrogenic Petri dishes (Corning, Lowell, MA, USA) at 37°C and 5% CO_2. The culture medium was replaced every 48–72 h and the cells were subcultured before they reached confluency.

The mIMCD-3 mouse inner medullary collecting duct cell line was obtained from the American Type Culture Collection (ATCC; Manassas, VA, USA) and cultured in DMEM/F12 (Gibco) supplemented with 10% FBS and Pen/Strep at 37°C and 5% CO_2 (Rauchman *et al*., 1993). The culture medium was replaced every 48–72 h and the cells were passaged before they reached confluency.

2.4. Tubule formation

To induce tubule formation, dispersed CMUB-1 or mIMCD-3 cells were suspended in collagen I gel and seeded in a micropatterned gel (Figure 1B, C). In brief, confluent CMUB-1 or mIMCD-3 cells were washed with PBS and detached from the culture dish using 0.05% trypsin–EDTA. After detaching, growth medium was added and the cells were centrifuged at 400 × *g* for 3 min. The cells were resuspended in growth medium and stored on ice. A collagen I solution (1.2–4.8%) was produced from rat tail collagen I concentrate (BD Bioscience, Bedford, MA, USA), according to the manufacturer's guidelines. Aliquots of CMUB-1 or mIMCD-3 cells were centrifuged (400 × *g*, 3 min), resuspended in liquid collagen I solution ($5–7 \times 10^6$cells/ml) and incubated on ice. 50 µl droplets of the dispersed CMUB-1 or mIMCD-3 cells suspended in collagen I were pipetted onto the micropatterned gels (Figure 2A) and incubated for 30–45 min at 4°C to allow the cells to settle into the pattern.

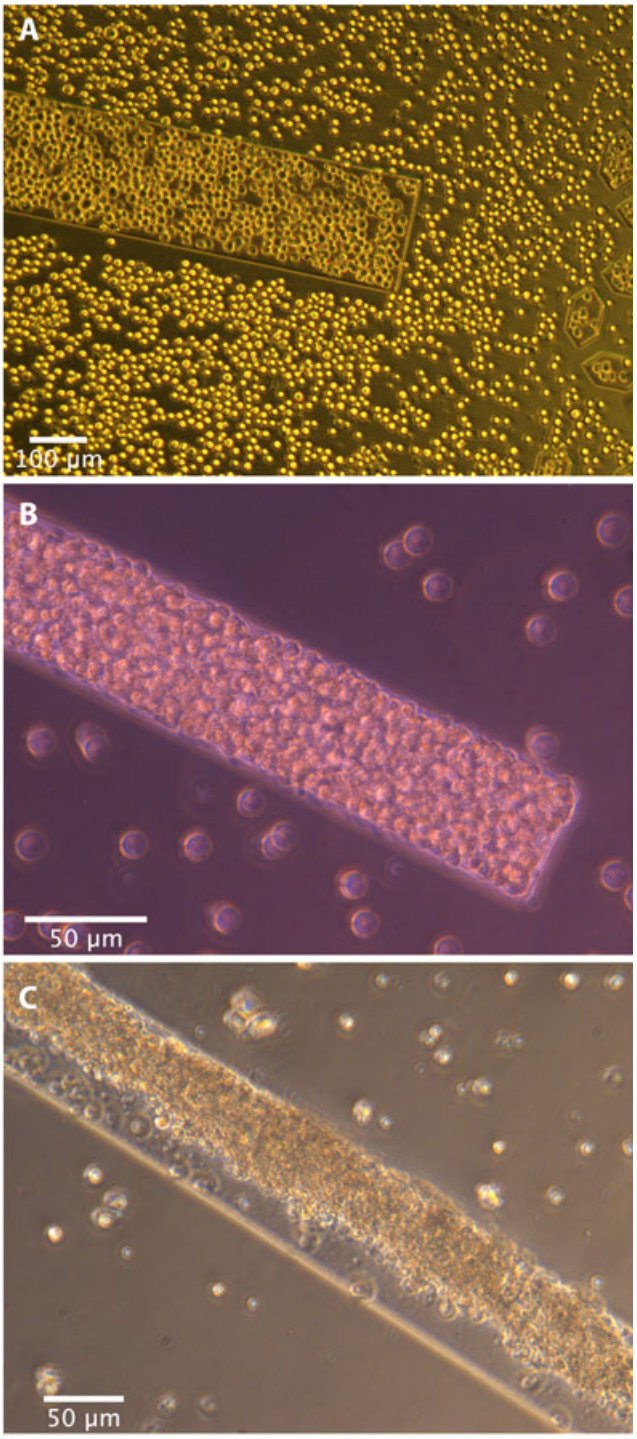

Figure 2. Cell seeding. Cells suspended in collagen I seeded on micropatterned gel (A). Excess cells were removed from the gel by centrifugation, forcing additional cells into the cavities (B). After 24 h, the dispersed single cells formed a tubular structure that conformed to the shape of the micropattern (C)

DOI: 10.1002/term

Subsequently, the micropatterned gels were centrifuged (600 rpm, 6 min, 4°C) in a microplate carrier (GS-6R, Beckman Coulter, Fullerton, CA, USA) to remove excess cells and liquid collagen I (Figure 2B). Optimal centrifugation conditions have been established by varying the centrifugation speed (200–800 rpm) and time (2–10 min). An optimal centrifugation angle of 90° of the mould cavities relative to the centrifugation axis was established by testing angles between 0° and 90°. The quality of the seeding procedure and the progress of tubule formation were observed by light microscopy (Figure 2C). The micropatterned gel holding the cells was then submerged in growth medium and incubated at 37°C and 5% CO_2. After 24–36 h, the tubes thus formed were gently removed from the micropatterned gel and used for subsequent experiments. Some tubes were incubated for extended periods of up to 7 days to allow for more extended lumen formation.

2.5. Growth factors and tube formation

The influence of growth factors and matrix components on tubule formation was tested by their addition to the growth medium and the collagen I suspension during tubule formation. Growth factors and matrix components were tested in four different concentrations, as follows: aldosterone, 10, 50, 100 and 200 nM (Sigma-Aldrich); bone morphogenic factor 7 (BMP7), 5, 10, 25 and 50 ng/ml (R&D Systems, Minneapolis, MN, USA); epidermal growth factor (EGF), 10, 20, 40 and 80 ng/ml (R&D Systems); fibroblast growth factor (FGF), 50, 100, 250 and 400 ng/ml (Sigma-Aldrich); fibronectin, 10, 20, 50 and 100 μg/ml (Sigma-Aldrich); hepatocyte growth factor (HGF), 10, 20, 50 and 100 ng/ml (Sigma-Aldrich); vascular endothelial growth factor (VEGF), 10, 20, 40 and 60 ng/ml (R&D Systems). To test each factor, cells were seeded onto 12 hydrogel moulds holding 10 or 20 cavities, and an average of 154.6 ± 19 or 154.8 ± 21 tube cavities, seeded with CMUB1 or mIMCD cells, respectively, were tested for each factor at different concentrations. To compare the effects of these factors, the number of formed tubes was counted after 24 h of culture and expressed as the percentage of the total number of cavities seeded.

2.6. *In vitro* budding

To induce budding *in vitro*, the tubes were exposed to growth factors, as described previously (Maeshima *et al.*, 2006). In brief, tubular structures were harvested from the moulds and transferred to 24-well plates by pipetting. The tubes were cultured in growth medium in the presence of 125 ng/ml glial cell-derived neurotropic factor (GDNF; R&D Systems) for 5–7 days. To induce budding, the tubes were placed next to follistatin-soaked beads, which were prepared by incubating Affi-Gel Blue Gel beads (Bio-Rad, Hercules, CA, USA) in follistatin (500 ng/ml in water; R&D Systems) for 4 h. Prior to use, the beads were rinsed quickly in sterile 1× PBS. To hold the tubes and beads in place, they were covered with a thin film of a 20% solution of matrigel (R&D Systems). GDNF-independent budding was induced similarly by exposing the tubes to growth medium containing 125 ng/ml fibroblast growth factor 7 (FGF7; R&D Systems) next to follistatin-soaked beads (500 ng/ml) for 5–7 days (Maeshima *et al.*, 2007). Pipettes with silicon-coated (Sigmacote®, Sigma) tips were used to transfer the tubular structures.

2.7. Immunohistochemical staining

Whole tubular structures were washed and stained in a 24-well plate. If necessary, antigen retrieval was performed by boiling the tubes in citrate buffer, pH 6.8. for 10–20 min, followed by incubation on ice. The tubes were stained with primary antibody overnight (PBS + 0.1% BSA, 4°C). The structures were washed [2 × 30 min, PBS, room temperature (RT)] and the fluorescently labelled secondary antibody (PBS + 0.1% BSA) was applied and incubated in the dark at RT for 4 h or overnight. After removing excess antibody by washing (2 × 30 min, PBS, RT), the structures were mounted on microscope slides (Superfrost Plus, Thermo Fisher Scientific, Waltham, MA, USA) with Vectamount (Vector Laboratories). The antibodies used were: anti-laminin antibody (1:300; Sigma-Aldrich); DBA fluorescent (1:400; Vector Laboratories); WT1 antibody (1:200; Dako); Anti-Ms IgG–$Alexa_{594}$ (1:400; Invitrogen); Anti-Rb-IgG–$Alexa_{594}$ (1:400; Invitrogen); and Anti-Rb-IgG–$Alexa_{488}$ (1:500; Invitrogen). Tubular structures were counterstained with diamino-2-phenylindole (DAPI) nuclear stain (Invitrogen, Carlsbad, CA, USA; 1 μg/ml, 10 min, RT) or DRAQ5 (Cell Signaling; 1 μM in PBS, 5 min, RT), followed by washing twice in PBS (10 min, RT).

2.8. Microscopy

Laser confocal fluorescence microscopy and 3D stack imaging was performed with an Olympus FV1000 microscope using Olympus Fluoview 3.1 software (Olympus, Center Valley, PA, USA). Cell culture images were taken with a Meiji TC5100 inverted microscope (Meiji Techno, San Jose, CA, USA), using Moticam 5.0 in combination with Motic Images 2.0 (Microscope World, Carlsbad, CA, USA).

3. Results

3.1. Seeding of cells

Cells were seeded into the cavities of the micropatterned gel by centrifugation. We tested centrifugation speeds in the range 200–800 rpm with varying times (2–10 min) and found that centrifugation at a speed of 600 rpm for 6 min at 4°C was the most suitable for even distribution of the cells and to remove excess cells from the surface of the gel. We also found that the orientation of the

DOI: 10.1002/term

micropatterned gel in the centrifuge greatly influenced the seeding efficiency. A 90° orientation of the micropattern relative to the centrifugation axis resulted in maximum efficiency. Orientation of the micropattern in angles between of 0–75° resulted in uneven cell distribution.

3.2. Formation of tubular structures

Based on our preliminary experiments, in which different sizes of the cavities in the micropatterned gel (width 30–225 μm, depth 50, 100 and 150 μm, length 3 or 6 mm) were tested, we found that cavities with a width of 50, 75, 100, 125 or 150 μm, a depth of 100 or 150 μm and a length of 3 or 6 mm were suitable for tubule formation, and these were used in further experiments. Time-lapse images of the cells in the micropatterned cavities were taken to demonstrate the dynamic process of tubule formation (Figure 3). At 1 h after seeding, CMUB-1 cells were packed into the 3D space of the gel's cavities as dispersed individual cells (Figure 3A); 10 h after seeding, the cells condensed into a rather uniform structure that conformed to the size and shape of the mould (Figure 3B). As shown in the image, parts of the structure started to contract and detach from the mould; 16 h after seeding, the structure detached further from the mould and formed a tubular structure (Figure 3C). This process continued at 20 and 24 h (Figure 3D, E). At 26 h after seeding (Figure 3F) we found that the whole generated tubular structure frequently detached from the mould. Tubular structures that did not detach completely could be removed from the mould by gentle pipetting.

3.3. Lumen formation

Confocal fluorescent microscopy demonstrated that the resulting tubular structures contained a lumen. Figure 4A shows a DAPI-stained tube where the lumen formation started at the tip of the tubular structure. The majority

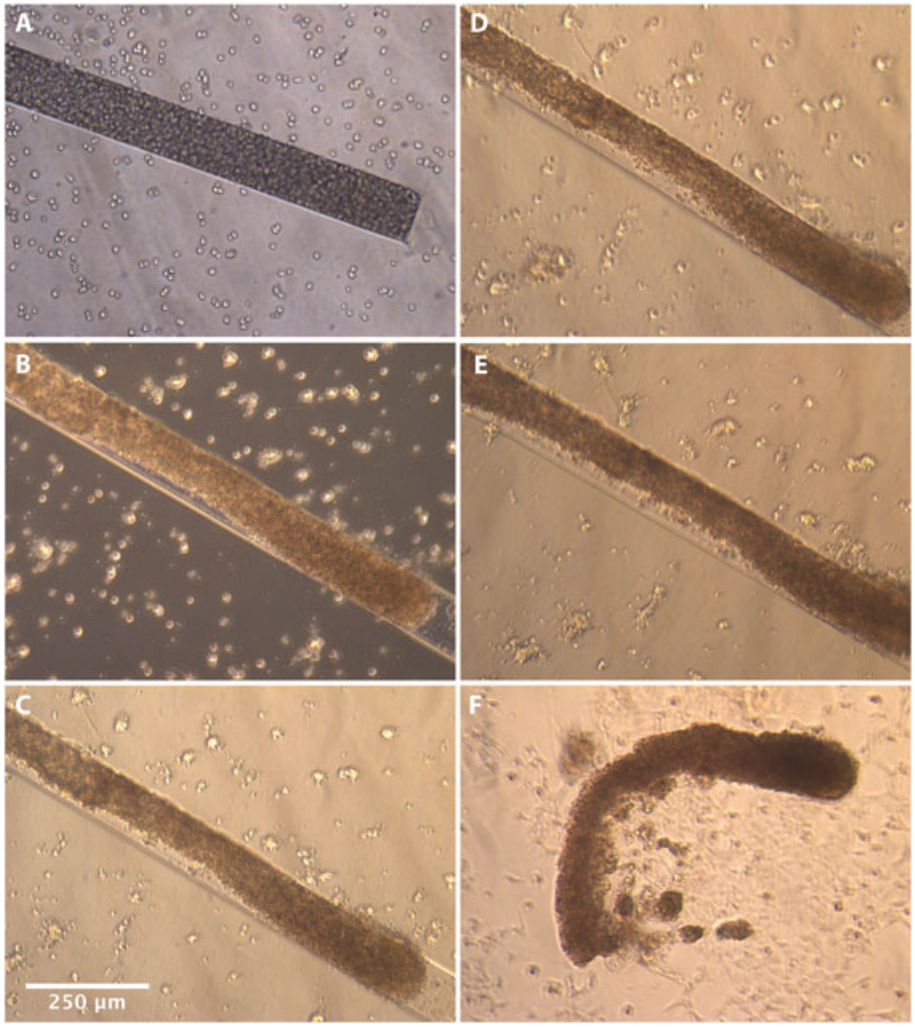

Figure 3. Time-lapsed sequence of tube formation; the dynamic change of CMUB-1 cells from individually dispersed cells to a tubular structure. Dispersed cells could be seen in the cavity at 1 h after seeding (A). After 10 h, a condensed structure was visible (B). Detachment of the structure started after 16 h (C) and continued at 20 h (D) and 24 h (E). After 26 h, the tubular structure detached completely from the mould (F)

DOI: 10.1002/term

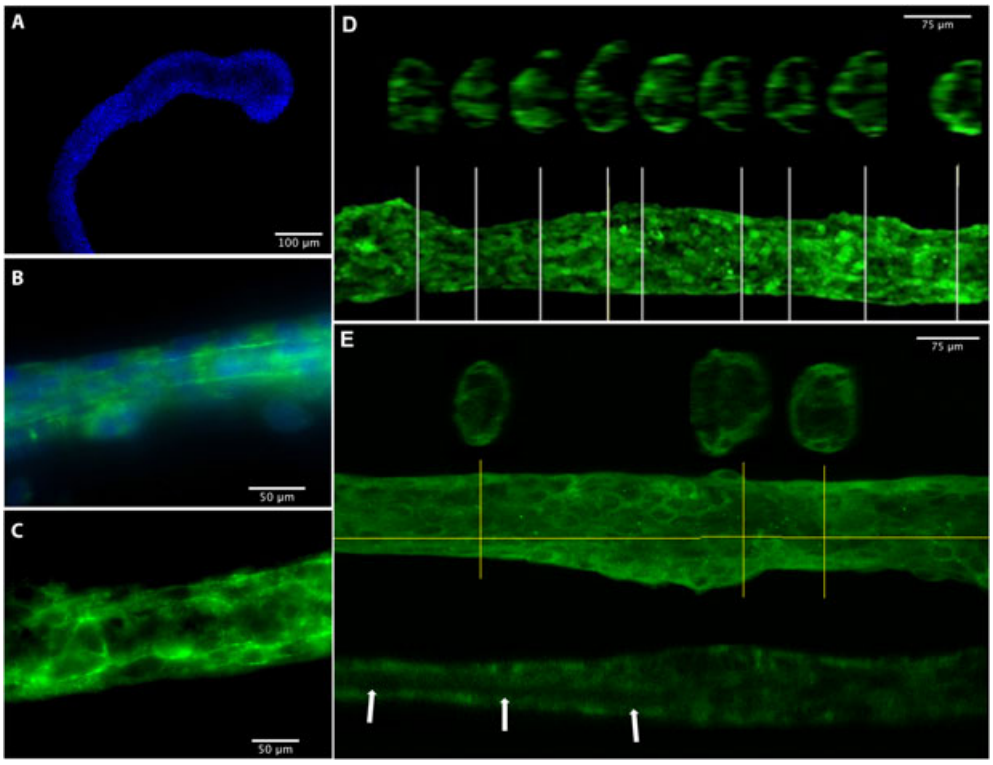

Figure 4. Tubular lumen. Confocal images of immunofluorescence (IF) stained mIMCD and CMUB-1 tubes demonstrate lumen formation. Nuclear staining (DAPI, blue) of a CMUB-1 tubular structure shows the initiation of lumen formation from one end of the tube (A). Laminin staining ($Alexa_{488}$, green) in combination with DAPI staining of a mIMCD tube demonstrates the linear structure along the lumen of the tube (B). *Dolichos biflorus* agglutinin (DBA) staining (green) of a mIMCD tube shows linear lining of cells along both sides of the tube (C). Virtual transverse cuts of a reconstructed z-stack of a CMUB-1 tube stained with laminin (green), taken 24 h after incubation, shows multiple developing luminal structures (D). Transverse and sagittal cuts of reconstructed z-stack of a CMUB-1 tube incubated for 7 days show more coalesced and extended tubular lumen (as indicated by arrows) (E)

of tubes were formed with single-cell layers lining the wall (Figure 4). However, tubes with multilayered cells were occasionally found, particularly in moulds with a cavity width $> 100\,\mu m$ (data not shown). Figure 4B depicts a laminin-stained (green) tubular structure with a mostly single-cell wall. The linear lumen border is clearly visible, and DAPI-stained nuclei (blue) are arranged along the tubular walls. Figure 4C shows a tubular structure stained with *Dolichos biflorus* agglutinin (DBA; green), which is a characteristic of the UB-derived tissue. Figure 4D shows a 3D reconstruction of z-stacks of a tubular structure with virtual cuts across the transverse axis of a CMUB-1 tube taken 24 h after incubation. The multiple lumina seen at different locations along the tube reflect the early stage of lumen formation before they coalesce to form a single lumen. The reconstructed z-stack of the sagittal virtual cut of a CMUB-1 tube that was incubated for a longer period of time (7 days) reveals the presence of a more coalesced lumen over a more extended tubule length (indicated by arrow, Figure 4E).

3.4. Influence of collagen I concentration on tubule formation

To test the influence of collagen I concentration on tubule formation, CMUB-1 cells were suspended in collagen I of different concentrations (1.2, 2.4, 3.6 or 4.8 mg/ml) (Figure 5A). We found that a collagen I concentration of 2.4 mg/ml resulted in the highest percentage of tubule formation (70% of 146 samples). A lower concentration of 1.2 mg/ml was slightly less efficient (61% of 140 samples). Increased concentrations of collagen I (3.6 and 4.8 mg/ml), hence more rigid gels, inhibited tubule formation (21% and 3% of 146 and 149 samples, respectively). Cells that were suspended in growth medium instead of collagen I did not stay in the micropattern of the agarose gels (0.5–4%) and were not viable (data not shown).

3.5. Influence of growth factors on tubule formation

To compare the influence of different growth factors on tubule formation, we cultured CMUB-1 and mIMCD cells in the micropatterned gels in the presence of different growth factors and counted the percentage of formed tubules after 24 h of culture. We found that in our culture system, tubule formation in CMUB-1 cells could be positively influenced by some growth factors. As shown in Figure 5B, CMUB-1 cells responded positively to aldosterone at low and high concentrations (10, 50 and 200 µg/ml), while no change in tubule formation was observed at 100 µg/ml. CMUB-1 cells also showed a tendency for a higher rate of tubule formation in the presence of FGF (50 and 100 µg/ml) and fibronectin (10 and 50 µg/ml),

DOI: 10.1002/term

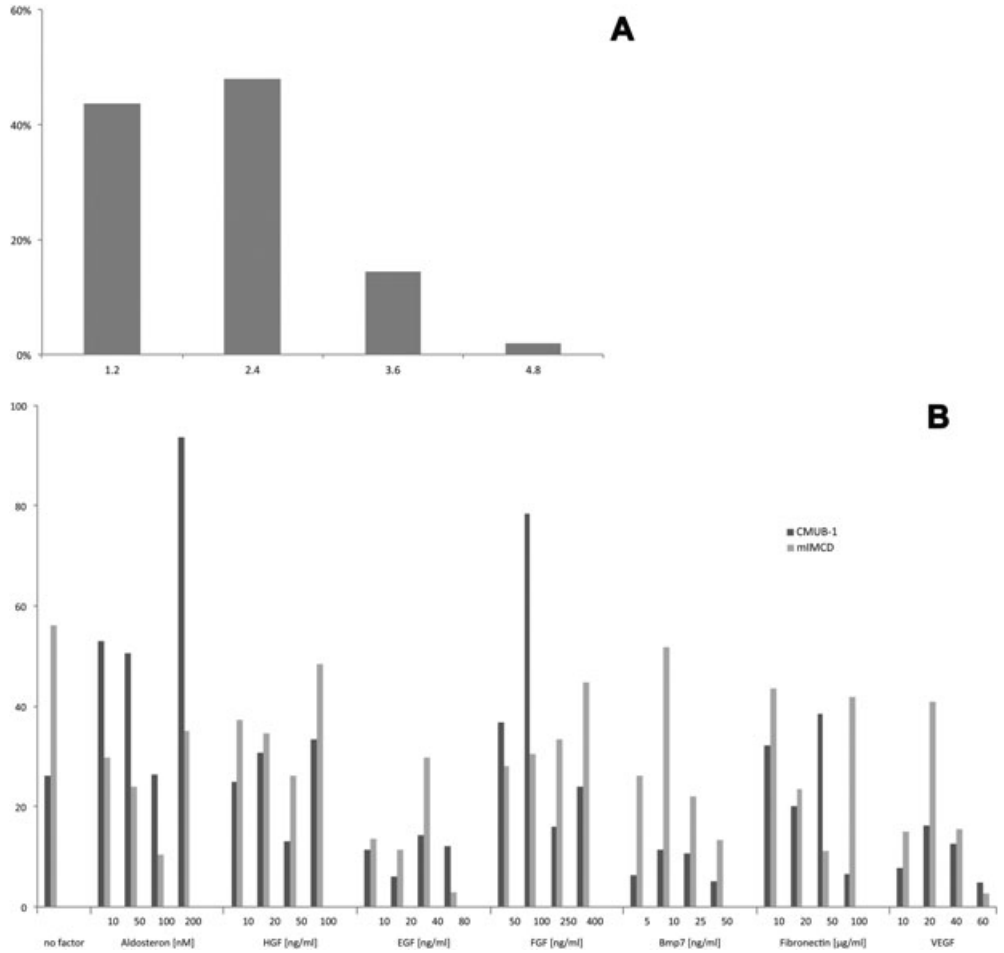

Figure 5. Factors influencing tube formation; results are presented as the percentage of total seeded cavities with tubule formed. (A) Influence of collagen I concentration on tubulogenesis of CMUB1 cells. Suspending cells in 2.4% collagen before seeding generated the highest number of tubes, as compared to 1.2%, 3.6% or 4.8%. (B) Growth factors (HGF, 10, 20, 50 and 100 ng/ml; EGF, 10, 20, 40 and 80 ng/ml; FGF, 50, 100, 250 and 400 ng/ml; BMP7, 5, 10, 25 and 50 ng/ml; VEGF, 10, 20, 40 and 60 ng/ml; Aldosterone, 10, 50, 100 and 200 nM; Fibronectin, 10, 20, 50 and 100 µg/ml) were added to both collagen I suspension (2.4%) and growth medium

while EGF, HGF, BMP7 and VEGF tended to reduce the rate of tubule formation (Figure 5B). mICMD cells, on the other hand, showed reduced tubule formation in the presence of most growth factors. Only the presence of high concentrations of HGF (100 ng/ml) and FGF (400 ng/ml) and a low concentration of BMP (10 ng/ml) and VEGF (20 ng/ml) did not interfere with tubule formation (Figure 5B).

3.6. Induction of budding *in vitro*

Previous studies have shown that ectopic budding from the Wolffian duct, a process that gives rise to UB during kidney development, can be induced by GDNF or FGF7 when the endogenous activin A activity is inhibited by follistatin (Maeshima *et al*., 2006, 2007). We tested whether budding of the tubular structures generated from mIMCD or CMUB-1 cells could be induced using the same signalling mechanism. As shown in Figure 6A–D, we found that exposure to culture medium containing GDNF (125 ng/ml) induced ectopic budding when activin A activity was inhibited locally by follistatin-soaked beads (500 ng/ml) that were placed next to the tubule. We did not observe budding in a control experiment, in which a BSA-soaked bead (1%) was used in combination with GDNF (Figure 6E). Alternatively, the same budding phenomenon could also be triggered by the exposure of the tubules to FGF7 (125 ng/ml)-containing medium and follistatin-soaked beads (500 ng/ml) (Figure 6F–H). When follistatin was added to the GDNF-containing medium, numerous buddings occurred on the tubes (Figure 6I, white arrows). In a control experiment, where a BSA-soaked bead (1%) was used in the presence of FGF7, the tubes did not show budding (Figure 6J). The ectopic buds outgrowing the generated tubular structure in the *in vitro* budding experiment were 18–55 µm in diameter. The length of the outgrowths was 50–400 µm and depended on the distance from the follistatin-soaked beads (Figure 6A–J). The deformation of tubes, likely due to contraction of the collagen I gel in the tubes after extended exposure to the medium, apparently had no visible influence on the budding process.

DOI: 10.1002/term

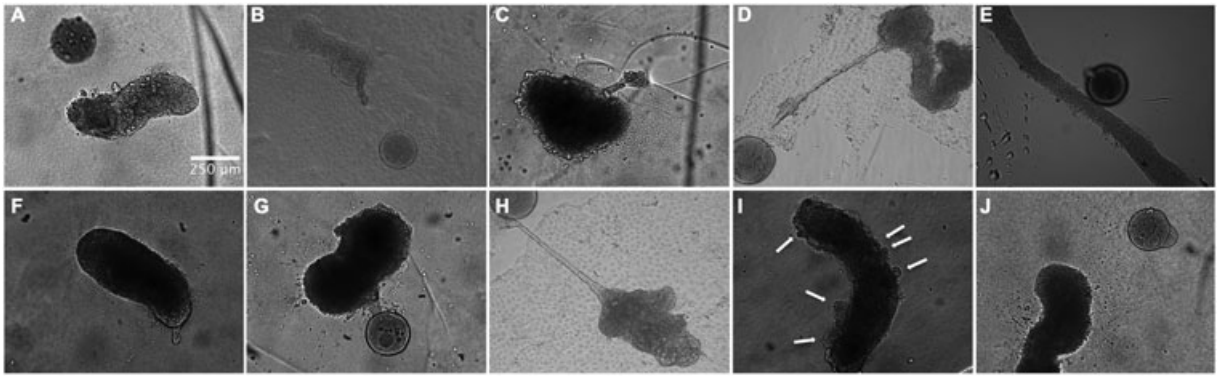

Figure 6. Ectopic budding. (A–D) Induction of budding of mIMCD tubes by the addition of 125 ng/ml GDNF to the growth medium, with follistatin-soaked beads (500 ng/ml) after days 1 (A), 3 (B), 5 (C) and 7 (D) in different samples. No budding was observed in a control experiment when tubes were exposed to GDNF-containing medium (day 7) (E). (F–H) Induction of budding of mIMCD tubes by the addition of 125 ng/ml FGF7 to the growth medium, with follistatin-soaked beads (500 ng/ml), after days 3 (F), 5 (G) and 7 (H). Addition of follistatin directly to GDNF-containing medium resulted in budding from multiple areas (day 5; indicated by white arrows) (I). In control experiments, in which tubes were exposed only to FGF7, which was added to the medium directly, no budding was observed (day 7) (J). Due to shrinking of the collagen I gel that was used to seed the cells, the tubes have lost their linear shape and appear coiled

4. Discussion

In this paper we report the generation of tubular structures with a micropatterned gel from two dispersed UB-derived cell lines: CMUB-1 cells, a cell line established from UB of the mouse embryonic kidneys (Ye *et al*., 2004); and mIMCD-3 cells, a cell line established from mouse terminal inner medullary collecting duct (Rauchman *et al*., 1993). Tubule formation from dispersed UB-derived cells has been described previously (De Filippo *et al*., 2002; Minuth *et al*., 2004; Orabi *et al*., 2012; Sakurai *et al*., 1997; Santos *et al*., 1993; Ye *et al*., 2004). In these experiments, growth factors, steroids, 3D culture, addition of extracellular matrix proteins, or special surfaces were used to promote tubule formation (De Filippo *et al*., 2002; Minuth *et al*., 2004; Orabi *et al*., 2012). However, in these studies, the tubule formation and branching occurred randomly, resulting in tubes of varying geometry and size. By using a micropatterned mould, as in our present study, we were able to generate tubes from dispersed UB cells with predetermined size and shape. The size of the micropatterned cavities was optimized to allow tubule formation and to generate tubular structures that largely resemble in size the Wolffian duct of the mouse embryo. The generated tubes had a diameter of 50–150 µm and a length of 3 or 6 mm, while the isolated Wolffian duct has a diameter of 70–120 µm and a length of 1.3–1.6 mm (Rosines *et al*., 2007).

Lumen formation has been described to involve processes of wrapping and budding of polarized cells or hollowing and cavitation of non-polarized cells (Andrew and Ewald, 2010). The mode of tubule formation in the micropatterned mould, however, is not clearly understood. We observed that tubule formation starts at one tip of the tube in the micropatterned mould (Figures 3B, 4A), although we cannot rule out the possibility that this could be attributed to a higher cell density at the end of the mould, due to a centrifugation artifact. The lumen formation in our method appears to be in the form of cord hollowing, a common mechanism for tube formation from dispersed cells, where agglomerated cells polarize and create small luminal spaces, which in later stages coalesce to become a larger single lumen (Andrew and Ewald, 2010). As shown in Figure 4D, 24 h after seeding CUMB-1 cells to the micropatterned mould, multiple small luminal spaces developed in the tubes. After longer incubation, these small luminal spaces began to coalesce to form a larger connected lumen, as shown in Figure 4E (connected lumen indicated by arrows).

The development of a tubular lumen (Figure 4A–E) is an important characteristic of the generated structures, as it is associated with the polarization of the epithelial cells. Hall *et al*. (1982) demonstrated that polarization and lumen formation can be induced *in vitro* by covering renal epithelial cells with ECM material. Others have also demonstrated lumen formation from endothelial cells in a 3D collagen matrix (Montesano *et al*., 1983). Nelson *et al*. (2008) were able to grow dispersed cells into geometrically defined shapes using a collagen I-based mould. In their experiments, cells were suspended in growth medium before being seeded into a collagen I-based mould, suggesting that the multiple contact sites of the cells in the collagen I mould are enough to induce morphogenesis. In preliminary experiments, we obtained similar results, where dispersed CMUB-1 cells suspended in growth medium without collagen I also formed tubes after they were seeded into the micropatterned gel (data not shown). The rate of tubule formation was, however, lower, mostly because of problems with not being able to hold the cells in the mould.

We found that higher concentrations of collagen I had a negative influence on tubule formation. This could be due to reduced cell mobility in the higher-concentrated, and therefore more rigid, collagen gel (Figure 5A). In our system, we also found that the addition of growth factors, such as HGF, EGF, FGF, BMP7, VEGF or aldosterone, or matrix protein such as fibronectin, did not dramatically

DOI: 10.1002/term

alter the tubule formation rate in UB-derived cells suspended in type I collagen. We found that, as compared to controls, both aldosterone (200 nM) and FGF (50 or 100 ng/ml) increased tube formation at high concentrations in CMUB1 cells, but not in mIMCD-3 cells (Figure 5B). While the exact mechanism underlying the non-linear response to aldosterone awaits further investigation, we suspect that this may be caused by the different binding affinities of aldosterone to mineralocorticoid receptor (MR), its main receptor, and to glucocorticoid receptor (GR), a secondary receptor (Claire *et al*., 1978; Fagart *et al*., 1998; Hellal-Levy *et al*., 1999). In the absence of glucocorticoid *in vitro*, aldosterone binds with high affinity to MR, so that aldosterone at low concentrations may stimulate MR only (Gaeggeler *et al*., 2005). At high concentrations, aldosterone may also bind to the GR and stimulate both receptors. Similar findings have also been reported for the binding of bFGF (Nugent and Edelman, 1992; Zhu *et al*., 2010). The positive effect of aldosterone on tube formation has been demonstrated previously by Minuth's group (Heber *et al*., 2007; Minuth *et al*., 2008); our results seem to be in variance with previous reports, where positive influences were found with these factors and matrices on tubule formation (Kloth *et al*., 1998; Minuth *et al*., 1993; Morimoto *et al*., 1994; Santos *et al*., 1993; Ye *et al*., 2004). The reason for such discrepancy is not immediately clear. It is possible that the confined space in the cavities of the micropatterned gels in which the tubules were formed could have impeded the tubule formation response to these factors. It is also possible that these factors did not have full accessibility to those cells embedded in collagen gel in the cavities.

In subsequent experiments, we examined the functionality of the generated tubes *in vitro* by testing their budding response to growth factors. During kidney development, UB develops through budding from the Wolffian duct in response to GDNF secreted from the surrounding MM (Little *et al*., 2010). Maeshima *et al*. (2006, 2007) were able to show that ectopic budding can be induced *in vitro* on isolated Wolffian ducts by GDNF or FGF7 when the endogenous activin A activity was suppressed by follistatin-soaked beads placed adjacent to the Wolffian duct. Activin A is a cytokine of the transforming growth factor-β (TGFβ) superfamily, and is involved in morphogenesis, angiogenesis and tissue repair (Cancilla *et al*., 2001; Maeshima *et al*., 2001; Poulaki *et al*., 2004). In the developing kidney, activin A influences the branching morphology by delaying branching and reducing the number of branching points (Ritvos *et al*., 1995). Follistatin is a TGFβ family antagonist and binds to activin A with high affinity (Harrison *et al*., 2006). Release of follistatin from the bead blocks local activin A activity, and allows branching induction by GDNF or FGF7. In our experiments, we found that tubes generated from dispersed mIMCD or CMUB-1 cells responded to GDNF or FGF7 by budding when local activin A was inhibited by follistatin released from the adjacent beads (Figure 6). The size of the ectopic buds from the generated tubes was similar in size to the size of the ectopic buds that were found on *in vitro*-cultured Wolffian ducts (Maeshima *et al*., 2007; Rosines *et al*., 2007). The budding structures in our experiment had diameters of 18–55 μm. In a Wolffian duct *in vitro* study, Rosines *et al*. (2007) showed ectopic buds with diameters of 70–120 μm, and Maeshima *et al*. (2007) showed diameters of 30–60 μm. In our current study, the average length of the outgrowth was 50–400 μm and depended on the distance from the follistatin-soaked bead (Figure 6A–J). This demonstrates the preservation of an *in vivo* functional characteristic of UB in tubes generated *in vitro* from dispersed UB-derived cells.

In summary, we described a method to generate tubular structures with a defined geometry and size from dispersed renal cells, using a predefined patterned microenvironment. The ability to induce tubule formation from dispersed renal progenitor cells with a micropatterned mould will be useful to generate elementary structures with a high similarity to the developing kidney. This represents the initial, and likely also an essential, part of a strategy to generate an embryonic kidney *in vitro*.

Conflict of interest

The authors declare no conflicts of interest.

Acknowledgement

This study was supported by generous funds provided by the Chau-Li Foundation (to N.Y.).

References

Andrew DJ, Ewald AJ. 2010; Morphogenesis of epithelial tubes: insights into tube formation, elongation, and elaboration. *Dev Biol* **341**: 34–55.

Basu J, Ludlow JW. 2012; Developmental engineering the kidney: leveraging principles of morphogenesis for renal regeneration. *Birth Defects Res C Embryo Today* **96**: 30–38.

Cancilla B, Jarred RA, Wang H *et al*. 2001; Regulation of prostate branching morphogenesis by activin A and follistatin. *Dev Biol* **237**: 145–158.

Claire M, Rafestin-Oblin ME, Michaud A *et al*. 1978; Statistical test of models and computerised parameter estimation for aldosterone binding in rat kidney. *FEBS Lett* **88**: 295–299.

De Filippo RE, Yoo JJ, Atala A. 2002; Urethral replacement using cell seeded tubularized collagen matrices. *J Urol* **168**: 1789–1792; discussion, 92–93.

Evenou F, Fujii T, Sakai Y. 2010; Spontaneous formation of stably-attached and 3D-organized hepatocyte aggregates on oxygen-permeable polydimethylsiloxane

membranes having 3D microstructures. *Biomed Microdevices* **12**: 465–475.
Fagart J, Wurtz JM, Souque A *et al*. 1998; Antagonism in the human mineralocorticoid receptor. *EMBO J* **17**: 3317–3325.
Gaeggeler HP, Gonzalez-Rodriguez E, Jaeger NF *et al*. 2005; Mineralocorticoid versus glucocorticoid receptor occupancy mediating aldosterone-stimulated sodium transport in a novel renal cell line. *J Am Soc Nephrol* **16**: 878–891.
Ganeva V, Unbekandt M, Davies JA. 2011; An improved kidney dissociation and reaggregation culture system results in nephrons arranged organotypically around a single collecting duct system. *Organogenesis* **7**: 83–87.
Hall HG, Farson DA, Bissell MJ. 1982; Lumen formation by epithelial cell lines in response to collagen overlay: a morphogenetic model in culture. *Proc Natl Acad Sci U S A* **79**: 4672–4676.
Harrison CA, Chan KL, Robertson DM. 2006; Activin-A binds follistatin and type II receptors through overlapping binding sites: generation of mutants with isolated binding activities. *Endocrinology* **147**: 2744–2753.
Heber S, Denk L, Hu K *et al*. 2007; Modulating the development of renal tubules growing in serum-free culture medium at an artificial interstitium. *Tissue Eng* **13**: 281–292.
Hellal-Levy C, Couette B, Fagart J *et al*. 1999; Specific hydroxylations determine selective corticosteroid recognition by human glucocorticoid and mineralocorticoid receptors. *FEBS Lett* **464**: 9–13.
Kloth S, Gerdes J, Wanke C *et al*. 1998; Basic fibroblast growth factor is a morphogenic modulator in kidney vessel development. *Kidney Int* **53**: 970–978.
Lenas P, Moos M, Luyten FP. 2009; Developmental engineering: a new paradigm for the design and manufacturing of cell-based products. Part II: from genes to networks: tissue engineering from the viewpoint of systems biology and network science. *Tissue Eng B Rev* **15**: 395–422.
Little MH. 2006; Regrow or repair: potential regenerative therapies for the kidney. *J Am Soc Nephrol* **17**: 2390–2401.
Little M, Georgas K, Pennisi D *et al*. 2010; Kidney development: two tales of tubulogenesis. *Curr Top Dev Biol* **90**: 193–229.
Maeshima A, Nojima Y, Kojima I. 2001; The role of the activin–follistatin system in the developmental and regeneration processes of the kidney. *Cytokine Growth Factor Rev* **12**: 289–298.
Maeshima A, Vaughn DA, Choi Y *et al*. 2006; Activin A is an endogenous inhibitor of ureteric bud outgrowth from the Wolffian duct. *Dev Biol* **295**: 473–485.
Maeshima A, Sakurai H, Choi Y *et al*. 2007; Glial cell-derived neurotrophic factor independent ureteric bud outgrowth from the Wolffian duct. *J Am Soc Nephrol* **18**: 3147–3155.
Minuth WW, Fietzek W, Kloth S *et al*. 1993; Aldosterone modulates PNA binding cell isoforms within renal collecting duct epithelium. *Kidney Int* **44**: 537–544.
Minuth WW, Sorokin L, Schumacher K. 2004; Generation of renal tubules at the interface of an artificial interstitium. *Cell Physiol Biochem* **14**: 387–394.
Minuth WW, Denk L, Castrop H. 2008; Generation of tubular superstructures by piling of renal stem/progenitor cells. *Tissue Eng C Meth* **14**: 3–13.
Montagne K, Komori K, Yang F *et al*. 2009; A micropatterned cell array with an integrated oxygen-sensitive fluorescent membrane. *Photochem Photobiol Sci* **8**: 1529–1533.
Montesano R, Orci L, Vassalli P. 1983; *In vitro* rapid organization of endothelial cells into capillary-like networks is promoted by collagen matrices. *J Cell Biol* **97**: 1648–1652.
Morimoto A, Tada K, Nakayama Y *et al*. 1994; Cooperative roles of hepatocyte growth factor and plasminogen activator in tubular morphogenesis by human microvascular endothelial cells. *Jpn J Cancer Res* **85**: 53–62.
Nelson CM, Vanduijn MM, Inman JL *et al*. 2006; Tissue geometry determines sites of mammary branching morphogenesis in organotypic cultures. *Science* **314**: 298–300.
Nelson CM, Inman JL, Bissell MJ. 2008; Three-dimensional lithographically defined organotypic tissue arrays for quantitative analysis of morphogenesis and neoplastic progression. *Nat Protoc* **3**: 674–678.
Nugent MA, Edelman ER. 1992; Kinetics of basic fibroblast growth factor binding to its receptor and heparan sulfate proteoglycan: a mechanism for cooperactivity. *Biochemistry* **31**: 8876–8883.
Orabi H, Aboushwareb T, Zhang Y *et al*. 2012; Cell-seeded tubularized scaffolds for reconstruction of long urethral defects: a preclinical study. *Eur Urol* **63**(3): 531–538.
Poulaki V, Mitsiades N, Kruse FE *et al*. 2004; Activin a in the regulation of corneal neovascularization and vascular endothelial growth factor expression. *Am J Pathol* **164**: 1293–1302.
Provin C, Takano K, Yoshida T *et al*. 2009; Low O2 metabolism of HepG2 cells cultured at high density in a 3D microstructured scaffold. *Biomed Microdevices* **11**: 485–494.
Raghavan S, Nelson CM, Baranski JD *et al*. 2010; Geometrically controlled endothelial tubulogenesis in micropatterned gels. *Tissue Eng A* **16**: 2255–2263.
Rauchman MI, Nigam SK, Delpire E *et al*. 1993; An osmotically tolerant inner medullary collecting duct cell line from an SV40 transgenic mouse. *Am J Physiol* **265**: F416–F424.
Reidy KJ, Rosenblum ND. 2009; Cell and molecular biology of kidney development. *Semin Nephrol* **29**: 321–337.
Ritvos O, Tuuri T, Eramaa M *et al*. 1995; Activin disrupts epithelial branching morphogenesis in developing glandular organs of the mouse. *Mech Dev* **50**: 229–245.
Rosines E, Sampogna RV, Johkura K *et al*. 2007; Staged *in vitro* reconstitution and implantation of engineered rat kidney tissue. *Proc Natl Acad Sci U S A* **104**: 20938–20943.
Rosines E, Johkura K, Zhang X *et al*. 2010; Constructing kidney-like tissues from cells based on programs for organ development: toward a method of *in vitro* tissue engineering of the kidney. *Tissue Eng A* **16**: 2441–2455.
Sakurai H, Barros EJ, Tsukamoto T *et al*. 1997; An *in vitro* tubulogenesis system using cell lines derived from the embryonic kidney shows dependence on multiple soluble growth factors. *Proc Natl Acad Sci U S A* **94**: 6279–6284.
Santos OF, Moura LA, Rosen EM *et al*. 1993; Modulation of HGF-induced tubulogenesis and branching by multiple phosphorylation mechanisms. *Dev Biol* **159**: 535–548.
Saxen L. 1987; Organogenesis of the Kidney. Cambridge University Press: Cambridge, London, New York, Melbourne, Sydney.
Schmidt-Ott KM, Lan D, Hirsh BJ *et al*. 2006; Dissecting stages of mesenchymal-to-epithelial conversion during kidney development. *Nephron Physiol* **104**: 56–60.
Unbekandt M, Davies JA. 2010; Dissociation of embryonic kidneys followed by reaggregation allows the formation of renal tissues. *Kidney Int* **77**: 407–416.
Ye P, Habib SL, Ricono JM *et al*. 2004; Fibronectin induces ureteric bud cells branching and cellular cord and tubule formation. *Kidney Int* **66**: 1356–1364.
Zhu H, Duchesne L, Rudland PS *et al*. 2010; The heparan sulfate co-receptor and the concentration of fibroblast growth factor-2 independently elicit different signalling patterns from the fibroblast growth factor receptor. *Cell Commun Signal* **8**: 14.

DOI: 10.1002/term